THE CURRENT–VOLTAGE CHARACTERIZATION OF THE Au/METHYLENE BLUE/GaAs ORGANIC-MODIFIED SCHOTTKY DIODES

Abdullah AKKAYA [*]

Chemistry and Chemical Processing Technology Department, Mucur Vocational College, Ahi Evran University, Kırşehir, Turkey

ABSTRACT

We report the electrical properties of the Au/n–GaAs devices with and without thin organic interface layer. Methylene blue (MB) is a heterocyclic aromatic chemical compound with the molecular formula C16H18N3SCl. The MB layer was formed by spin coating technique on chemically cleaned gallium arsenide (GaAs) substrate. The current–voltage ($I–V$) characteristics of the Au/MB/n–GaAs metal-insulator-semiconductor (MIS) and Au/n–GaAs metal-semiconductor (MS) devices have been investigated at room temperature. The MS and MIS devices $I–V$ characteristics showed a good rectification, and they were analyzed based on the thermionic emission (TE) theory. The ideality factor (n) and the barrier height ($\Phi_b^{(IV)}$) from the $I–V$ characteristics was determined as 1.131±0.006 and 0.782±0.005 eV for MS device and 1.336±0.057 and 0.950±0.008 eV for MIS device, respectively. A Cheung's method and modified Norde's function has been used to extract the parameters including the (Φ_b) and the series resistance (R_S).

Distributions of the interface state density (D_{it}) of the MS and MIS devices were derived from $I–V$ measurements. Our results indicate that the Au/MB/n–GaAs device had lower interface state density values than the Au/GaAs device. Also non-saturated reverse bias current was investigated by the using a Pole-Frenkel emission model. Furthermore, the optical and morphological properties of MB layer were investigated by the Atomic Force Microscopy (AFM), Scanning Electron Microscopy (SEM) and UV-vis Spectrophotometer (UV-vis).

Finally, we showed that, increasing Φ_b and decreasing D_{it} and improving electrical parameters of MIS devices indicates that, thin MB interface layer could be prefer for modification of Au/n–GaAs devices.

Keywords: Metal-interfacial layer-semiconductor structures, Methylene Blue; Schottky barrier, Series resistance, Interface states

1. INTRODUCTION

The devices fabricated on GaAs have a great importance both in micro- and opto-electronic applications. Because, GaAs MS and MIS devices are used as a basic component for low power devices, high speed electronic and optoelectronic [1-4]. Also, modified GaAs devices with the organic interlayer, it is well known that, using an interface layer between the metal and the semiconductor, can be easily changed by the electrical properties and parameters of the contacts and also these interlayers can be easily manufactured by relatively inexpensive techniques such as dipping, spin coating and printing.[2, 4-10]. Therefore, many researchers focused on modification of GaAs MS devices with the organic interlayer to reveal the properties and exact description of current transport mechanism in contacts [2-15]. Researchers were used a different type polymeric or non-polymeric organic compounds as an interface layer such as poly(2-methoxy-5-(2/-ethyl-hexyloxy)-1,4-phenylene vinylene) (MEH-PPV) [2], Rhodamine 101 [5], poly(3,4-ethylenedioxithiophene)-block-poly(ethylene glycol) (PEDOT) [6], perylene-monoimide (PMI) [7], Rhodamine-B (RhB) [8], 3,4,9,10-perylene tetra carboxylic dianhydride (PTCDA) [9], octadecylthiol (ODT) [10], N,N′-dimethyl-3,4,9,10-perylene tetra carboxylic diimide (DiMe-PTCDI) [13], dicarboxylic acid derivatives [14], phenol red [15], rubrene [16] and etc.

*Corresponding Author: abdullah.akkaya@ahievran.edu.tr

Generally, main purpose of inserting organic interlayer between semiconductor and metal was enhancement of the device performance. In other words; thin organic layer may be used to control the electrical characteristics of conventional MS structures, by way of the selection of different organic molecules and, changing the thickness of interlayer, the device can be shaped or designed to show some desired properties. Conjugate organic materials have a growing interest because of their potential easy processing, low-cost applications, great chance to modify their chemical structures and good harmony with a variety of substrates. Kampen et al. [9] and Zahn et al. [13] have used DiMe-PTCDI and PTCDA to modify Schottky contacts on GaAs. They were determined barrier heights from their *I-V* measurements, and in most cases, the values of obtained barrier heights are larger than that of conventional metal/GaAs contacts. Vilan et al. [14] was used monolayer of small molecules to control Au/GaAs diodes. By using a few of multifunctional molecules, which these molecule dipoles were varied systematically, they produced diodes with a barrier height that is tuned by the molecular dipole moment. Vural et al. [5] and Soylu et al. [8] was investigated that the temperature dependent electrical characteristics of interfacial layer with Rhodamine derives.

MB was a heterocyclic aromatic chemical compound available as a dark blue powder soluble in water and ethyl alcohol and widely used as a redox indicator, peroxide generator or sulfide analysis in chemistry, cell marking in biology, medical care of some poisoning and, disease in medicine because of redox indicator and dye properties (see inset in Figure 1). In this study, we were used MB to fabricate a GaAs MIS for investigate the effect of MB layer on some typical metal-semiconductor device parameters of Au/GaAs device by using *I-V* measurements. The characteristic diode parameters such as barrier height and ideality factor obtained from the individual *I-V* and *C-V* characteristics were compared with each other.

2. EXPERIMENTAL

In this work, n-type LEC GaAs wafer was used with a wafer surface orientation (100), Te-doped, front side polished and back side as cut/etched. The doping concentration of wafer was $2\text{-}5 \times 10^{17}$ cm^{-3} and grown by the LEC method. The wafer was chemically cleaned from organic residues, using trichloroethylene (TCE), acetone ((CH3)2CO) and methanol (CH3OH) for 5 min., respectively, in ultrasonic bath. Next, for the 60 s, the wafer was dipped in HF:H_2O (1:10) solution to eliminate any thin native oxide layer on the surface. After that, wafer rinsed in de-ionized water of 18.2 MΩ-cm, dried with high-purity N_2 gas and inserted into the deposition chamber. Ohmic contact metal, Au-Ge alloy (%12 wt.), was deposited, by using a thermal evaporation method, on the whole non-polished side of the wafer with a thickness of 200 nm, under the vacuum of 1×10^{-6} Torr, and then wafer was thermally annealed in a quartz tube furnace at 350 °C for 2 min. in N_2 ambient. Thereafter, the wafer was cut into two pieces of 5x5 mm each. The MB layer was formed on polished side of one of them by the using 5 mM MB solution (prepared with the de-ionized water) with spin coating. Spin coating time was 60 s at 5000 rpm on a spin coater (Süss Delta6 RC). With and without the MB layered samples were inserted into the evaporation chamber. Thickness of MB layer was 12.8 nm and measured by AFM. A high purity Au metal (99.995%) was deposited by rapid thermal evaporation method through the molybdenum shadow mask. The thickness of Schottky contacts metal were 30 nm, deposition rate was 1nm per second and monitored by QCM.

Electrical measurements of fabricated devices were carried out using a HP 4140B pA meter SMU, at room temperature and in dark. All measurement and data evaluation procedures was performed via Agilent VEE Pro virtual engineering software based our computer program SeCLaS [17, 18].

3. RESULTS AND DISCUSSION

3.1. Optical and Structural Features of MB Thin Film

When considering optical band gap of materials, correct information is required for several practical applications such as solar cell applications of dyes. MB is a cationic dye and exhibits two main absorption bands at 293 nm ($\pi-\pi*$) and 665 nm with the shoulder at 610 nm ($n-\pi*$) (n is the free doublet of S atom on S=C bond and free doublet on the nitrogen atom of C=N bond) in diluted aqueous solutions [19-21]. The absorption (*A*) and transmission (*T*) spectra of the MB thin film in the spectral range of 200–1100 nm was shown in Figure 1. In this spectra, absorption peaks were widened because of the thickness of the film, semitransparent film spin coated with the same condition of MIS devices, normally UV-vis spectra taken from diluted (around the 5nM) solutions in quartz cells.
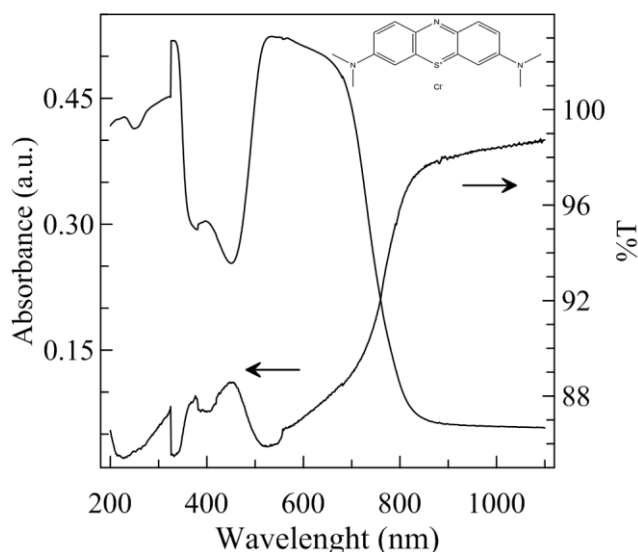
**Figure 1.** UV-vis spectra of MB. Inset show that the molecular structure of the *MB*.

The absorption band gap of the MB thin film was determined from the absorbance spectra data and Tauc relation. The optical absorption coefficient (α) value was calculated from the following equation [22];

$$\alpha = 2.303 A/d \tag{1}$$

where *d* is film thickness (12.8 nm) and *A* is the optical absorbance. In here, α related with the band gap of molecule having the parabolic band structure. The allowed direct band gap or absorption band gap value of the organic thin film was determined via Tauc relation [22];

$$\left(\alpha h \vartheta\right)^{n} = K\left(h\vartheta - E_{g}\right) \tag{2}$$

where *n* is a constant and could be taken 1/2, 3/2, 2 and 3 for direct allowed, direct forbidden, indirect allowed and indirect forbidden transitions, respectively. *K* is a constant depended on the transition probability, *hv* and E_{g} are photon energy and the optical band gap energy, respectively. Dominated transition was allowed direct transition thus a value of *n* = 2 was found to be most suitable for the MB thin film. Figure 2 is show a plot of *(αhv)²* versus *hv* for the MB samples on quartz substrates. The E_{g} value was obtained as 1.62 eV by extrapolating the linear part of the photon energy axis with the help of Equation (2).
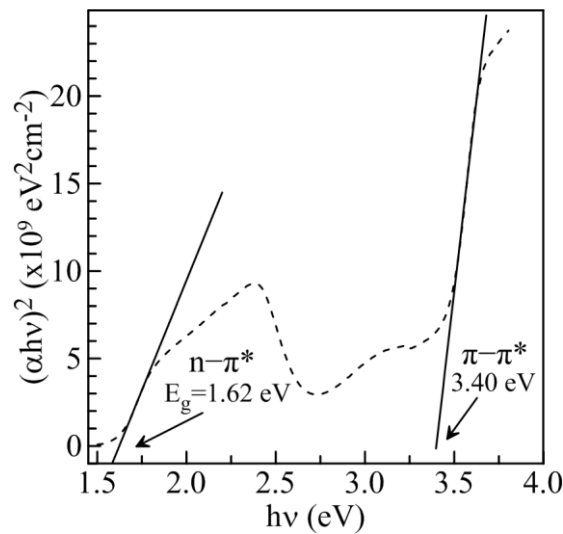
Figure 2. *(αhν)²* vs. *hν* graphs of the MB.

First absorption band was corresponded to (n→π*) excitation, which equal to forbidden bandgap, with the 1.62 eV energy. Second absorption band was corresponded to (π→π*) excitation with the 3.40 eV energy.

Surface topography, thickness and roughness of MB thin film on GaAs substrate was investigated using AFM. Determined root-mean-square (RMS) or roughness for MB thin film was a 2.081 nm and thickness was a 12.8 nm (Figure 3).
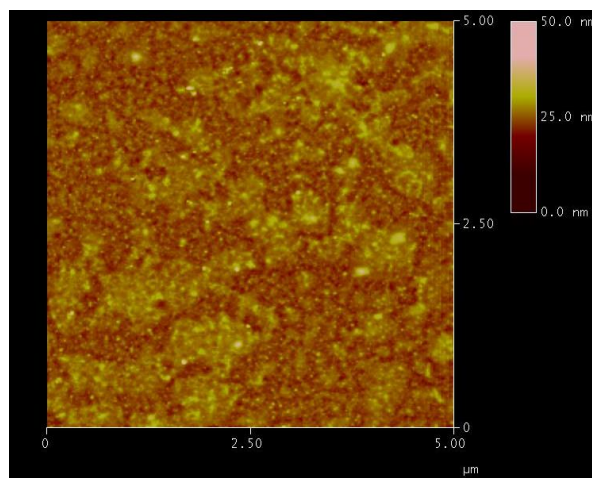
Figure 3. AFM image of MB layer on GaAs substrate.

SEM was used to study the surface morphology, shape and size of the grain, thickness of MB thin film on GaAs substrate. Figure 4 clearly shows that the film was uniformly spread all substrate surface. Also, small spherical grains and non-uniform cracks exist on film surface. Information about the average grain size and cracks was determined by analyzing the SEM images using ImageJ software. According to this analyze, average spherical grain size, domain size and width of crack was a 17.41 nm, 321 nm and 15.04 nm, respectively.
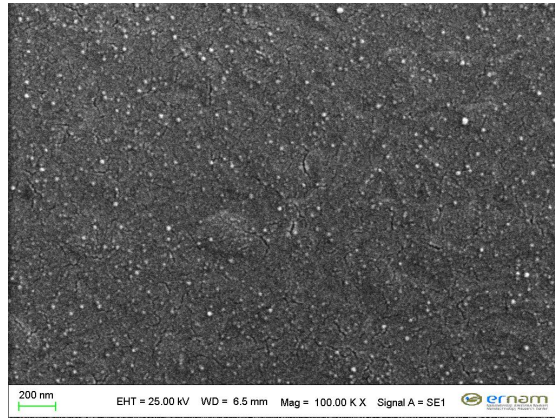
Figure 4. SEM image of MB layer on GaAs substrate.

3.2. Analysis of Forward Bias I-V Characteristics of Fabricated MS and MIS Devices
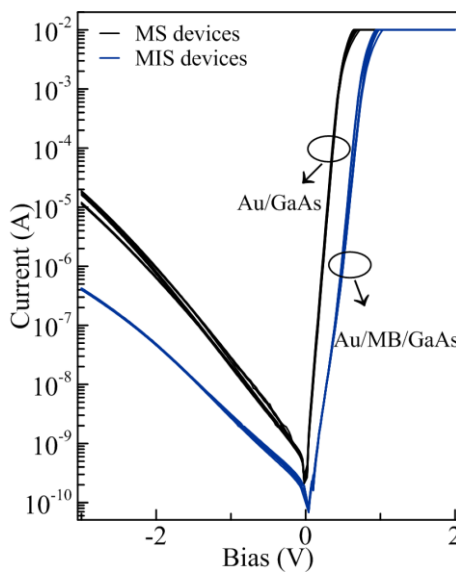
Typical *I-V* characteristics of Au/GaAs MS and Au/MB/GaAs MIS devices were shown in Figure 5. *I-V* characteristics of all devices have a good rectifying property. Analysis of *I-V* characteristics may be done in terms of TE theory. According to this theory, current through the diode is given by [23]

$$I = I_o \exp\left(\frac{qV}{nkT}\right) \tag{3}$$

Where, saturation current (I_o) is given by

$$I_o = AA^*T^2 \exp\left(-\frac{q\Phi_b^{(IV)}}{kT}\right) \tag{4}$$

where k is Boltzmann constant, n is ideality factor, which is a measure of the consistency of the diode to pure thermionic emission, q is electron charge, T is absolute temperature, V is applied bias, A^* is effective Richardson constant (8.16 Acm^{-2}K^{-2} for n-GaAs), A is effective diode area, and $\Phi_b^{(IV)}$ is barrier height. I_o, $\Phi_b^{(IV)}$ and n values were calculated from the slope of straight line part of the forward bias *lnI-V* plots and using with Equation (3) and Equation (4).

Figure 5. *I-V* characteristics of Au/GaAs and Au/MB/GaAs devices, at room temperature and in the dark.

Even if they were identically prepared, values of diode parameters for both MS and MIS devices were varied from diode to diode. When considering 10 diodes, the statistical analysis yields a mean barrier height and the ideality factor value for MS and MIS diodes and findings were summarized in Table 1. Also, homogenous barrier heights ($\Phi_b^{(H)}$) calculated from n-$\Phi_b^{(IV)}$ graph and its values were 0.815 eV and 0.996 eV for MS ($\circ$) and MIS ($\diamond$) devices, respectively (Figure 6a-b).
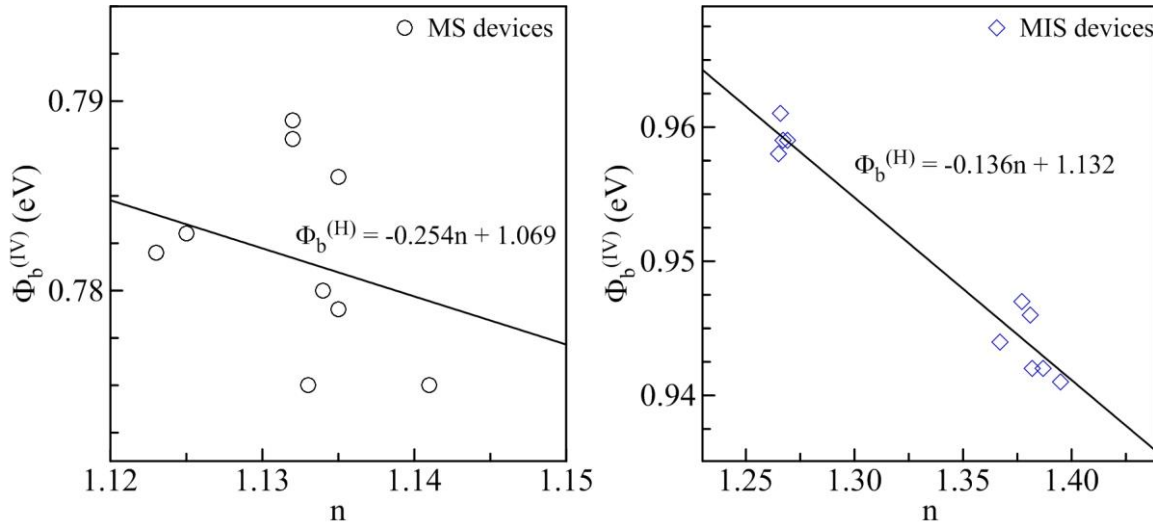

Figure 6. n vs. $\Phi_b^{(IV)}$ graphs of Au/GaAs (a) and Au/MB/GaAs (b) devices

Both diode's (MS and MIS) ideality factors was higher than the ideality (or unity), possibly cause of the presence of an unwanted natively grown oxide layer with different thickness from diode to diode, non-uniform distribution of the interfacial charges, generation-recombination processes, image force lowering and interface states in valance band which was equilibrium with the semiconductor, according to the model of Card and Rhoderick [24, 25]. Ideality factor of MIS diodes was greater than that for the MS diodes as expected [24, 26].

Table 1. Characteristics diode parameters (with standard deviations) of the Au/GaAs and Au/MB/GaAs devices obtained from I-V graphics. Each value represents the average of ten diodes.

MS/MIS	n	$\Phi_b^{(IV)}$ (eV)	Cheung				Norde	
			n	Rs (Ω)	Φ_b (eV)	Rs (Ω)	Φ_b (eV)	Rs (Ω)
Au/GaAs	1.131 ($\pm$0.006)	0.782 ($\pm$0.005)	1.038 ($\pm$0.064)	16.685 ($\pm$2.101)	0.815 ($\pm$0.030)	16.862 ($\pm$1.989)	0.830 ($\pm$0.007)	13.902 ($\pm$1.219)
Au/MB/GaAs	1.336 ($\pm$0.057)	0.950 ($\pm$0.008)	1.325 ($\pm$0.162)	15.408 ($\pm$2.982)	0.958 ($\pm$0.057)	15.446 ($\pm$2.932)	1.125 ($\pm$0.020)	14.062 ($\pm$4.242)

The mean $\Phi_b^{(IV)}$ for Au/GaAs MS device was close agreement with the reported values before [27, 28] in the literature. The mean $\Phi_b^{(IV)}$ for MIS device was greater than 163 meV that for the reference diode. This $\Phi_b^{(IV)}$ value for MIS devices better than the reported values of Vural et al. [5] and Şimşir et al. [7]. As reported in Reference [3], increment in $\Phi_b^{(IV)}$ value could be attributed to existence of the organic dye layer, changed the barrier height by affecting the space-charge region of the inorganic substrate.

It is well known that the effect of series resistance distinct from the interface states at sufficiently high voltages which it's in equilibrium with the semiconductor was cause by the downward concave tilt in the forward bias *I-V* plots [29]. The Φ_b as well as other diode parameters such as n and R_S is also determined using the Cheung's functions [29],

$$\frac{dV}{d(\ln I)} = IR_s + n\frac{kT}{q} \qquad (5)$$

$$H(I) = V - n\frac{kT}{q}\ln\left(\frac{I}{AA^*T^2}\right) \tag{6}$$

and

$$H(I) = IR_s + n\Phi_b^{(C)} \tag{7}$$

where $dV/d(lnI)$, $H(I)$ and $\Phi_b^{(C)}$ is Cheung functions. Equation (5) and Equation (7) gives a straight line for the data of downward curvature region in forward bias I-V characteristics. The y-axis slope and intercept of a plot of $dV/d(lnI)$ vs. I are provide R_s and nq/kT respectively. Using the n value in Equation (6) and a plot of $H(I)$ vs. I (according to Equation (7)) also gives a flat line with the y-axis intersect equal to $n\Phi_b^{(C)}$. Also, slope of this plot could be used in the calculation of second R_s value. Findings were summarized in Table 1.

Barrier height ($\Phi_b^{(N)}$) and series resistance (R_s) values of MS and MIS devices was also determined by using the Norde method [30]. In this method, the Norde function is expressed by

$$F(V) = \frac{V}{\gamma} - \frac{kT}{q}\ln\left(\frac{I}{AA^*T^2}\right) \tag{8}$$

and

$$\Phi_b^{(N)} = F(V_{\min}) + \frac{V_{\min}}{2} - \frac{kT}{q} \tag{9}$$

where $F(V_{min})$ is the minimum value of Norde function $F(V)$, V_{min} corresponding voltage and γ is first integer greater than n. $\Phi_b^{(N)}$ and R_s values were summarized in Table 1.

3.1. Analysis of reverse bias region of I-V characteristics

Also, non-saturated reverse current (I_R) characteristics of MS and MIS devices at moderate and low bias values was shown in the Figure 5. Poole–Frenkel emission (PFE) and Schottky emission (SE) models were used to investigate reverse leakage current mechanism of MS and MIS devices. Theoretical values of field lowering coefficients of both model is given by [31-33]

$$\beta_{PFE} \cong 2\beta_{SE} = \left(\frac{q^3}{\pi\varepsilon_0\varepsilon_r}\right)^{1/2} \tag{10}$$

β_{SE} and β_{PFE} are SE and PFE field lowering coefficients, respectively. ε_0 and ε_r dielectric constants of free space and dynamic dielectric constant, respectively. For MIS devices, the β_{PFE} was 8.530×10^{-6} eVm$^{1/2}$V$^{-1/2}$ (ε_r was taken 0.5 from [34]) and For MS devices the β_{PFE} was 3.412×10^{-5} eVm$^{1/2}$V$^{-1/2}$. PFE current is described as

$$I_R = I_o\exp\left(\frac{\beta_{PFE}V_R^{1/2}}{kTd^{1/2}}\right) \tag{11}$$

If, Schottky emission is dominant mechanism for reverse bias current, current is given by [31-33]

$$I_R = AA^*T^2\exp\left(-\frac{q\Phi_b^{(RB)}}{kT}\right)\exp\left(\frac{\beta_{SC}V_R^{1/2}}{kTd^{1/2}}\right) \tag{12}$$

where, $\Phi_b^{(RB)}$, V_R and d are reverse bias barrier height, reverse bias voltage and thickness of interfacial layer, respectively. The plot of $ln(I_R)$ vs. $V_R^{1/2}$ for the one MS and MIS devices were presented in Figure 7. In this figure, linear fit on $ln(I_R)$ vs. $V_R^{1/2}$ graph of MS devices (○) revealed that the mean

value of experimental β_{PFE} was $6.998\pm0.396 \times 10^{-6}$ eVm$^{1/2}$V$^{-1/2}$ and it was close to theoretical values of β (β_t). So, in reverse bias region, PFE was a dominant current conduction mechanism to the MS devices (Table 2.). Also, two different linear fit on $ln(I_R)$ vs. $V_R^{1/2}$ graph of MIS devices (◊) revealed that the two experimental β_{PFE} value was obtained and these values indicated that two emission mechanism exist in here. At that case, field lowering coefficients were calculated $2.616\pm0.307 \times 10^{-5}$ eVm$^{1/2}$V$^{-1/2}$ and $2.286\pm0.017 \times 10^{-5}$ eVm$^{1/2}$V$^{-1/2}$ at low and high reverse bias region respectively. These field lowering coefficient values were close to theoretical values of β_{PFE} and β_{SE} respectively. So, PFE was a dominant conduction mechanism at lower reverse bias region (between the -1.64 V and -1.80 V) and SE was a main current conduction mechanism at higher reverse bias region (between the -2.00 V and -3.00 V) (findings summarized in Table 2.).
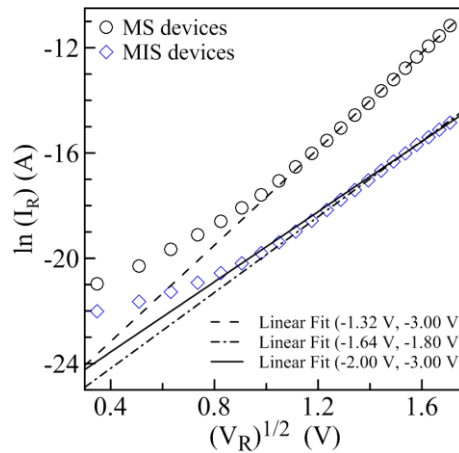
Figure 7. $ln(I_R)$ vs. $V_R^{1/2}$ graph of MS devices Au/GaAs and Au/MB/GaAs devices. Two regions appear in Au/MB/GaAs devices graph, indicates that the existence of additional current conduction mechanism.

Table 2. SE and PFE parameters (with standard deviations). Each value represents the average of ten diodes.

MS/MIS	$\Phi_b^{(RB)}$ (eV)	Emission model	I_0 (A)	β_{PFE} (eVm$^{1/2}$V$^{-1/2}$)	β_t (eVm$^{1/2}$V$^{-1/2}$)
Au/GaAs	0.747 ± 0.011	PFE	$1.839\pm0.777 \times 10^{-9}$	$6.998\pm0.396 \times 10^{-6}$	8.530×10^{-6}
Au/MB/GaAs	0.773 ± 0.029	PFE (Low V_R)	$5.110\pm0.316 \times 10^{-9}$	$2.616\pm0.307 \times 10^{-5}$	3.412×10^{-5}
	0.759 ± 0.001	SE (High V_R)	$1.032\pm0.039 \times 10^{-9}$	$2.286\pm0.017 \times 10^{-5}$	

These results suggested that the dominant field enhanced carrier transport in MS and MIS (low reverse bias region) devices was a PFE and carrier transport performed from the metal into the dislocations must occur via a trapped interface state instead of by direct thermal emission from the Schottky metal. However, field enhanced carrier transport in MIS devices was a SE and carrier transport occur via a direct thermal emission from the metal at high reverse bias region [35, 36].

3.4. Determination Density of Interface States of Fabricated Devices

3.4.1. Determination from I-V measurements

Barrier height of MS and MIS contacts is strongly correlated with the electric field in the space-charge region, thus, also depend on bias. The presence of an interfacial layer, Φ_e is assumed to be bias-dependent. Thus, effective barrier (Φ_e) could be defined in place of $\Phi_b^{(IV)}$ and written as follow [24];

$$\Phi_e = \Phi_b^{(IV)} + \left(\frac{d\Phi_e}{dV}\right)V = \Phi_b^{(IV)} + \beta V \tag{18}$$

where $d\Phi_e/dV$ is bias dependent coefficient and given by

$$\frac{d\Phi_e}{dV} = \beta = 1 - \frac{1}{n}.$$ (19)

According to the Card and Rhoderick [24], ideality factor becomes bigger than unity, when the device having interface states in equilibrium with the semiconductor, and density of interface states $D_{it}^{(IV)}$ is given by

$$D_{it}^{(IV)} = \frac{1}{q}\left[\frac{\varepsilon_i}{d}[n(V)-1] - \frac{\varepsilon_s}{w_d}\right]$$ (20)

where $n(V)$ is bias dependent ideality factor. The values of $D_{it}^{(IV)}$ were obtained via substituting voltage dependence values of ideality factor in Equation (20), using with d=0.5 nm, ε_i=13.1 and d=12.8 nm ε_i=6.18 [34] for MS and MIS devices. Figure 8 shows the curves of $D_{it}^{(IV)}$ determined from the experimental forward bias *I-V* graphics of Au/GaAs MS and Au/MB/GaAs MIS devices. As can be seen from Figure 8, exponential increment in $D_{it}^{(IV)}$ values, from midgap towards the bottom of conduction band were apparent for both MS and MIS devices at higher biases. $D_{it}^{(IV)}$ was a $1.103\pm0.032\times10^{12}$ eV^{-1}cm^{-2} (at V=0.3 V) and $5.151\pm1.266\times10^{10}$ eV^{-1}cm^{-2} (at V=0.5 V) for MS and MIS devices, respectively. $D_{it}^{(IV)}$ values of MIS devices was approximately 20 times lower than MS devices. This situation could be ascribing to the deactivation of substrate interface states by organic dye layer.
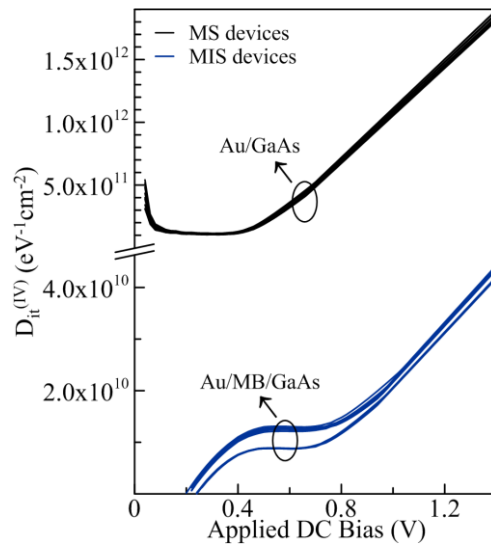
Figure 8. The energy distribution of interface states of MS and MIS devices.

The interface states were act as a generation-recombination center and, cause a reducing of the carrier life time and, a raise of the leakage currents and device noise. This phenomenon was related with threshold voltage shift and explained theoretically and experimentally by the dipolar contribution of molecule and charge transfer barrier in interface layer [43, 44]. Also, significant drop of $D_{it}^{(IV)}$ values of MIS devices at low biases was indicated that the pinned excess charges exist in MB layer. They were changed the position of donor like traps in the interior side of MB layer and created a fixed positive charge barrier. In other words, positively charged MB molecule were, which it's neutralized by the free chlorine ions in a solution, created a charge-transfer dipole at the MB layer-semiconductor interface. Firstly, electron affinity of any surface was directly affected by a surface dipole, which creates an electrical potential drop across the grafted molecular film depending on dipole moment. Secondly, mobile charges were primarily near the bottom of channel, this does not add significant additional resistance, but it does influence the local band bending through the charge-transfer dipole at the

interface. This was a main mechanism for reduction of $D_{it}^{(IV)}$ in MIS device at low biases. Magnitude of the $D_{it}^{(IV)}$ for MS and MIS devices was in close agreement with the literature [6, 45].

4. CONCLUSIONS

In this paper, optical and structural properties of MB thin film and, electrical properties of the Au/GaAs devices with and without MB layer were investigated by using UV-vis, AFM, SEM, *I-V* measurements. Forbidden band gap of MB film was a 1.62 eV. Film was a very smooth (RMS value is 2.081 nm) and uniformly spread all substrate surface.

Barrier height values were found as 0.950±0.008 eV and 0.782±0.005 eV for devices with and without the MB layer from *I-V* characteristics, respectively. This enhancement in barrier height was attributed to the organic dye layer shifting the effective barrier height as reported in literature. So, this modification method was "the way of the barrier height enhancement" with an approximately 168 meV between the barrier heights of MS and MIS diodes. Series resistances of the fabricated devices were obtained from Cheung functions combined with their forward *I-V* characteristics. Also, concluded that, the reverse bias current conduction mechanism was effected from the existence of MB layer between the Schottky metal and GaAs at higher reverse bias region. It was seen that the interface state density values of the Au/MB/GaAs device were lower than that of the Au/GaAs device. The reduction in interface state density values was attributed to passivation of interface state by organic dye layer.

ACKNOWLEDGEMENTS

REFERENCES

[1] Chang CY, Kai F, GaAs High-Speed Devices: Physics, Technology, and Circuit Applications. Wiley, 1994.

[2] Kundu S, Kumar A, Banerjee S, Banerji P. Electrical properties and barrier modification of GaAs MIS Schottky device based on MEH-PPV organic interfacial layer. Mat Sci Semicon Proc 2012; 15: 386-392.

[3] Vearey-Roberts AR, Evans DA. Modification of GaAs Schottky diodes by thin organic interlayers. Appl Phys Lett 2005; 86:

[4] Zahn DRT, Park S, Kampen TU. Tuning Schottky barrier heights by organic modification of metal-semiconductor contacts. Vacuum 2002; 67: 101-113.

[5] Vural O, Safak Y, Altındal S, Türüt A. Current-voltage characteristics of Al/Rhodamine-101/GaAs structures in the wide temperature range. Curr Appl Phys 2010; 10: 761-765.

[6] Aydın ME, Soylu M, Yakuphanoglu F, Farooq WA. Controlling of electronic parameters of GaAs Schottky diode by poly(3,4-ethylenedioxithiophene)-block-poly(ethylene glycol) organic interlayer. Microelectron Eng 2011; 88: 867-871.

[7] Şimşir N, Şafak H, Yüksel ÖF, Kuş M. Investigation of current–voltage and capacitance–voltage characteristics of Ag/perylene-monoimide/GaAs Schottky diode. Curr Appl Phys 2012; 12: 1510-1514.

[8] Soylu M, Yakuphanoglu F. Barrier height enhancement and temperature dependence of the electrical characteristics of Al Schottky contacts on p-GaAs with organic Rhodamine B interfacial layer. Superlattice Microst 2012; 52: 470-483.

[9] Kampen T et al. Schottky contacts on passivated GaAs(100) surfaces: barrier height and reactivity. Appl Surf Sci 2004; 234: 341-348.

[10] Dorsten J, Maslar J, Bohn P. Near-surface electronic structure in GaAs (100) modified with self-assembled monolayers of octadecylthiol. Appl Phys Lett 1995; 66: 1755-1757.

[11] Farag AAM, Yahia IS. Rectification and barrier height inhomogeneous in Rhodamine B based organic Schottky diode. Synthetic Met 2011; 161: 32-39.

[12] Yahia IS, Farag AAM, Yakuphanoglu F, Farooq WA. Temperature dependence of electronic parameters of organic Schottky diode based on fluorescein sodium salt. Synthetic Met 2011; 161: 881-887.

[13] Zahn DRT, Kampen TU, Mendez H. Transport gap of organic semiconductors in organic modified Schottky contacts. Appl Surf Sci 2003; 212: 423-427.

[14] Vilan A, Ghabboun J, Cahen D. Molecule-metal polarization at rectifying GaAs interfaces. J Phys Chem B 2003; 107: 6360-6376.

[15] Bobby A, Shiwakoti N, Gupta P, Antony B. Barrier modification of Au/GaAs Schottky structure by organic interlayer. Indian Journal of Physics 2015: 1-6.

[16] Tugluoglu N, Caliskan F, Yuksel OF. Analysis of inhomogeneous barrier and capacitance parameters for Al/rubrene/GaAs (100) Schottky diodes. Synthetic Met 2015; 199: 270-275.

[17] Akkaya A, Karaaslan T, Dede M, Çetin H, Ayyıldız E. Investigation of temperature dependent electrical properties of Ni/Al0.26Ga0.74N Schottky barrier diodes. Thin Solid Films 2014; 564: 367-374.

[18] Akkaya A, Esmer L, Kantar BB, Cetin H, Ayyildiz E. Effect of thermal annealing on electrical and structural properties of Ni/Au/GaN Schottky contacts. Microelectron Eng 2014; 130: 62-68.

[19] Párkányi C, Boniface C, Aaron JJ, Maafi M. A quantitative study of the effect of solvent on the electronic absorption and fluorescence spectra of substituted phenothiazines: evaluation of their ground and excited singlet-state dipole moments. Spectrochimica Acta Part A: Molecular Spectroscopy 1993; 49: 1715-1725.

[20] Heger D, Jirkovsk J, Kln P. Aggregation of Methylene Blue in Frozen Aqueous Solutions Studied by Absorption Spectroscopy. The Journal of Physical Chemistry A 2005; 109: 6702-6709.

[21] Cenens J, Schoonheydt R. Visible spectroscopy of methylene blue on hectorite, laponite B, and barasym in aqueous suspension. Clays and Clay Minerals 1988; 36: 214-224.

[22] Tauc J, Amorphous and liquid semiconductors. New York: Plenum Press, 1974.

[23] Rhoderick EH, Williams RH, Metal-Semiconductor Contacts. Oxford: Clarendon Press 1988.

[24] Card HC, Rhoderick EH. Studies of tunnel MOS diodes I. Interface effects in silicon Schottky diodes. Journal of Physics D: Applied Physics 1971; 4: 1589.

[25] Tung RT, Sullivan JP, Schrey F. On the Inhomogeneity of Schottky Barriers. Mat Sci Eng B-Solid 1992; 14: 266-280.

[26] Sze S, Physics of Semiconductor Devices. New York: John Wiley & Sons, 1981.

[27] Özdemir AF, Türüt A, Kökçe A. The double Gaussian distribution of barrier heights in Au/GaAs Schottky diodes from I–V–T characteristics. Semicond Sci Tech 2006; 21: 298-302.

[28] Leroy WP, Opsomer K, Forment S, Van Meirhaeghe RL. The barrier height inhomogeneity in identically prepared Au/GaAs Schottky barrier diodes. Solid State Electron 2005; 49: 878-883.

[29] Cheung SK, Cheung NW. Extraction of Schottky Diode Parameters from Forward Current-Voltage Characteristics. Appl Phys Lett 1986; 49: 85-87.

[30] Norde H. A modified forward I-V plot for Schottky diodes with high series resistance. J Appl Phys 1979; 50: 5052-5053.

[31] Reddy VR, Manjunath V, Janardhanam V, Kil YH, Choi CJ. Electrical Properties and Current Transport Mechanisms of the Au/GaN Schottky Structure with Solution- Processed High-k BaTiO3 Interlayer. J Electron Mater 2014; 43: 3499-3507.

[32] Kumar AA et al. Electrical properties of Pt/type Ge Schottky contact with PEDOT: PSS interlayer. J Alloy Compd 2013; 549: 18-21.

[33] Reddy VR. Electrical properties and transport mechanisms of Au/Ba0. 6Sr0. 4TiO3/GaN metal–insulator–semiconductor (MIS) diode at high temperature range. Applied Physics A 2016; 122: 1-7.

[34] Murthy V, Rao TP, Sobhanadri J. Dielectric properties of some dyes in the radio-frequency region. Journal of Physics D: Applied Physics 1977; 10: 2405.

[35] Lin J, Banerjee S, Lee J, Teng C. Soft breakdown in titanium-silicided shallow source/drain junctions. Electron Device Letters, IEEE 1990; 11: 191-193.

[36] Janardhanam V et al. Temperature dependency and carrier transport mechanisms of Ti/p-type InP Schottky rectifiers. J Alloy Compd 2010; 504: 146-150.

[37] Vasudevan S et al. Controlling transistor threshold voltages using molecular dipoles. J Appl Phys 2009; 105: 093703.

[38] Bahuguna A et al. Probing molecule-semiconductor interfaces through Metal Molecule Semiconductor transport characteristics. arXiv preprint arXiv:0912.1682 2009:

[39] Hudait MK, Krupanidhi SB. Interface states density distribution in Au/GaAs Schottky diodes on n-Ge and n-GaAs substrates. Mat Sci Eng B-Solid 2001; 87: 141-147.